International Journal of Engineering

Journal Homepage: www.ije.ir

Mass Production and Growth Mechanism of Carbon Nanotubes in Optimized Mechanothermal Method

S. O. Mirabootalebi*, G. H. Akbari, R. M. Babaheydari

Department of Materials & Metallurgy, Shahid Bahonar University of Kerman, Kerman, Iran

P A P E R I N F O

Paper history:
Received 8 May 2021
Received in revised form 8 August 2021
Accepted 24 August 2021

Keywords:
Carbon Nanotubes
Multi-walled Carbon Nanotubes
Synthesis of Carbon Nanotubes
Growth Mechanism of Carbon Nanotubes
Mechanothermal Method
Mass Production of Carbon Nanotubes

A B S T R A C T

There are a lot of major parameters in the mechanothermal approach such as milling time, ball-to-powder weight ratio (BPR), and cup speed which play a key role in the quality and quantity of the carbon nanotubes (CNTs). In this study, these essential factors in the mechanothermal method were optimized to maximize the efficiency of the process, and also the growth mechanism of CNTs was investigated. For these purposes, the milling of graphite was performed in a high alloy steel vial (Standard No. 1.2550 key-to-steel) for 330 h at the vial speed of 300 rpm in a planetary ball mill. The morphology and crystal structures of the graphite powder during the mechanical activation were studied by x-ray diffraction (XRD), Zeta-Sizer, and scanning electron microscope/energy-dispersive x-ray spectroscopy (SEM/EDX). After the heat treatment of amorphous carbon at 1400 ˚C, the CNTs were synthesized and their quality and quantity were analyzed by transmission electron microscopy (TEM), atomic force microscopy (AFM), XRD, Raman spectroscopy, and differential thermal analysis/thermogravimetric analysis (DTA/TGA). A special type of tip-growth mechanism based on the motion of the catalyst particles was proposed regarding the TEM images. According to this mechanism, the diameter, length, and shape of the CNT are completely dependent on a random motion of the catalyst particle at the tip of the nanotube. As a consequence, the growth mechanism in the mechanothermal process does not follow a certain pattern and this is the main reason for the spring-like and curved shape of the nanotubes. Furthermore, results of the differential thermal analysis revealed that the yield of fabricated multi-walled carbon nanotubes (MWCNTs) is more than 97% of the precursor.

***doi**: 10.5829/ije.2021.34.10a.14*

1. INTRODUCTION

The main methods for the production of carbon nanotubes are arc discharge [1], laser ablation [2], chemical vapor deposition (CVD) [3], electrolysis [4], and mechanothermal [5]. In the CVD and flame approaches, a high weight percentage of metal impurities is usually produced which required complex purification steps. Laser ablation, electrolysis, and arc discharge are suitable methods for the synthesis of high-quality CNTs, although they are not suitable for mass production and they need special equipment.

Mechanothermal is a simple and economic method for the large-scale generating of carbon nanotubes without producing a lot of metal impurities [6, 7]. Most of the generated CNTs in this way are bamboo and spring shape of MWCNTs with several millimeters in length [8, 9]. In the mechanothermal technique, graphite powder is milled and changed to amorphous carbon, and then in the annealing step, the carbon nanotubes are formed [10]. Indeed, the ball-milling and heat-treatment act as the nucleation and growth step, respectively [11]. The first mechanothermal method for synthesizing CNT was reported in 1999 by Chen et al. [12]. Then, Manafi et al. [9, 13] performed precise analyses to show the high capacity of this procedure for the fabrication of high-quality CNTs. Next, Guler et al. [14] generated carbon nanotubes in the shortest possible time and they developed the method.

Major parameters in the ball milling such as the time of milling by making the suitable precursor play an important role in the mechanothermal process for the

*Corresponding Author Institutional Email: oveis@eng.uk.ac.ir (S. O. Mirabootalebi)

Please cite this article as: S. O. Mirabootalebi, G. H. Akbari, R. M. Babaheydari, Mass Production and Growth Mechanism of Carbon Nanotubes in Optimized Mechanothermal Method, International Journal of Engineering, Transactions A: Basics Vol. 34, No. 10, (2021), 2332-2340

production of carbon nanotube [15]. On the one hand, structural defects and metal particles, which enter the powder during the milling, act as the catalysts for the formation of carbon nanotubes. Consequently, milling in an agate vial has a much lower efficiency for the production of CNTs than steel vial [16]. So, an increase in the volume of metal catalysts is equal to an increase in the yield of the process. On the other hand, the purification of the CNTs, in this case, becomes more difficult. In addition, high vial speed and milling time can lead to producing crumples of graphite sheets that are very stable and rarely converted to the tubular structure of CNT after the annealing step. Moreover, the temperature of the heat treatment is the other effective variable that should be in a certain range (1000-1800˚C) at the annealing step [10, 16]. This temperature is about half of the melting temperature of pure graphite, which leads to the formation of a tubular hollow structure of carbon .

In this research, all the mentioned effective factors from previous researches were adjusted to promote the efficiency of the process. First, the milling time, which is usually about 180 hours in the mechanothermal methods, was increased to 330 hours. As mentioned earlier, the metallic compounds of the vial that enter the powder during mechanical alloying are high potential regions for nucleation and growth of CNTs. Hence, a long milling time (330 h) and a high-alloy steel cup (Standard No 1.2550 key-to-steel) are selected for the mechanical activation step in this work. Most of the previous studies had utilized only one size of the balls [7, 15, 17], but using different dimensions of balls leads to a more random movement of balls and also more energy is transferred to the particles. Plus, the thickness of the powders layer on the surface of the balls and heterogeneity of the powders will be minimized [18]. So, we employed various sizes of balls to optimize the grinding process. As well as, what is not yet clear is the growth mechanism of CNTs in the mechanothermal method. In this paper, we also argue about the growth conditions of the nanotubes during the process.

Accordingly, the main purpose of the present work are the large-scale production of high-quality CNTs by applying the optimized factors and studying the growth mechanism of the carbon nanotubes.

2. MATERIALS AND METHODS

High purity graphite powder (15 μm size of flakes) was chosen as the precursor. The ball milling was carried out in a high-alloy steel vial (Standard No 1.2550 key-to-steel) at atmospheric pressure with 5 and 32 steel balls of 15 and 10 mm, respectively. The milling time was 330 h and BPR was kept at 20:1. The milling procedure was induced in a high-energy planetary ball mill under Argon at the cup speed of 300 rpm. In the next step, the ball-milled powders were placed in a furnace tube at 1400 ˚C for three hours in Argon to generate the CNTs. Finally, the obtained samples were placed in the furnace under the air atmosphere at the temperature of 330 ˚C for 132 min.

The structures of samples were studied by an X-ray diffractometer (Philips X'Pert, Cu-Kα, λ=0.1542 nm). Rietveld/MAUD refinement was used to measure the crystallite characteristics of the samples. The size distribution of the ball-milled graphite was measured by a zeta-seizer (ZEN3600). The morphologies of milled graphite particles were characterized by a scanning electron microscope (Cam Scan mv2300). The structure and size of the CNTs were analyzed by atomic force microscope (Autoprobe Cp, contact mode, 1 Hz rate of scan) and transmission electron microscope (LEO912-AB operated at 100 kV). The Raman spectroscopy (Takram P50C0R10, at 532 nm of laser wavelength) for analyzing the carbon nanotubes was carried out and DTA/TGA analyses (PC Luxx-NETZSCH) was taken in the air atmosphere to examine the mass loss profile and the thermal properties of the products.

3. RESULTS AND DISCUSSION

Figure 1 shows the XRD patterns of graphite particles during the ball milling process. There is a sharp and a broad peak at 26˚-27˚ and 43˚-46˚, respectively. These peaks are disappeared completely after the mechanical activation. The stable hexagonal phase is transformed gradually to the disordered and metastable amorphous phase and a noticeable reduction in crystallite size has occurred.

By increasing the activating times, both of the main peaks become broader because of the growing surface area of graphite particles, increasing and developing dislocations, creating sub-grain boundaries, and forming smaller grains. If the graphite grain size is reduced to about 3 nm, the crystal structure of graphite will transfer to the amorphous phase and this is related to the destruction of the graphite crystalline structure [12]. Based on the XRD profiles in Figure 1, the percentage of the produced amorphous phase, crystallite size, d002, the micro-strains were estimated by MAUD/Rietveld refinement, and then, these crystallographic data were put in Table 1.

The stable hexagonal close-packed (hcp) structure of carbon was still the dominant phase within the first 50 h of activation time. After 100 h of the ball-milling, the rate of destruction of the crystalline structure significantly decreased. Previous studies [13, 19] pointed out that no changes in the XRD pattern and the crystallite size have been observed after 170-1000 h of activation time. This is due to the creation of a balance between dislocation motion and recovery and recrystallization; thus cross slip does not cause the decrease in the grain size [18]. Actually, graphite sheets bent and converted to new

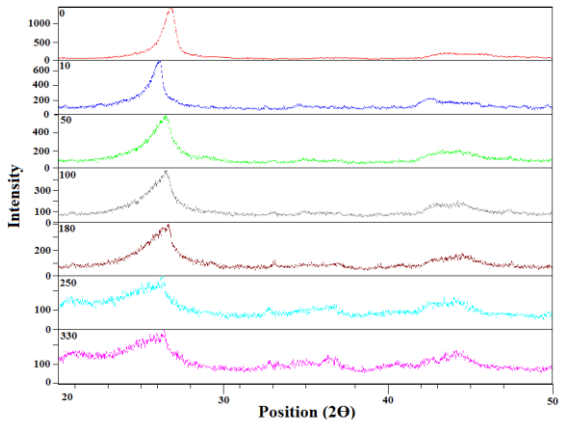

Figure 1. XRD patterns of graphite particles at different milling times

TABLE 1. The crystallographic data of graphite particles at different activation times

Milling Time (h)	Amorphous Phase (%)	Crystallite Size (nm)	d002 (nm)	Micro Strain (με)
0	0	390	0.332	0.00613
10	19	210.3	0.341	0.012
50	22	96	0.337	0.0175
100	69	58	0.337	0.0219
180	72	50.92	0.3376	0.0223
250	91	1.3	0.339	0.02507
330	93	1.3	0.339	0.02507

carbon-based nanostructures instead of a reduction in the crystallite size, owing to the high tenacity and flexibility of graphene plates and very strong σ bonds. These structures including carbon micro-tubes and carbon nanotubes [20, 21], ribbon nanostructures [22], and spherical and crustal structures of graphite [21]. Crumpled graphene sheets, hardly converted to nanotubes in the heat treatment stage due to high thermodynamic stability, toughness, and flexibility of the layers.

A key aspect of mechanical activation is the production of the amorphous phase as the precursor instead of these crumpled morphologies that are created at high milling speeds. In this study, instead of applying a high rotational speed, the normal speed (300 rpm) with high milling time was chosen to increase the percentage of the produced amorphous phase. As a result, we achieved to smallest crystallite size compared to similar works [6, 7, 23]. By increasing the milling time which leads to a long time of the process in the laboratory scale. This time can be reduced and the amount of initial graphite injected into the ball mill can be increased in order to achieve greater profitability by using industrial mills.

Generally, oxygen is slowing down the destructive process due to creating the saturated compounds with H_2, CO_2, and O_2, [24, 25]. In other words, Argon accelerates the reduction of the carbon grain size than Hydrogen and Oxygen under the same condition owing to its neutral nature [20].

The size distribution of the activated graphite for 330 h in a zeta-sizer analysis is depicted in Figure 2. The particle size distribution is in the range of 90-170 nm and the average particle is about 122 nm. The long-time of ball-milling transfers a high amount of energy to graphite particles which activation in all regions leads to the very fine and a none-wide distribution of the particles. This size distribution can facilitate the formation of the CNTs at the annealing step, since the uniform and very small particles by increasing the concentration gradient, have a positive impact on the formation of nanotubes.

Figure 3 illustrates the images of the scanning electron microscope of the initial graphite and the ball-milled graphite. The appearance of the spherical and the smaller graphite particles at 330 h of milling indicates structural changes and increasing the surface area of graphite particles due to high impact forces and severe plastic deformation. These ultra-activated turbostratic and amorphous particles with a high degree of agglomeration and free energy are the precursor materials and can be very effective on the quality and quantity of the CNTs which will be produced at the annealing step.

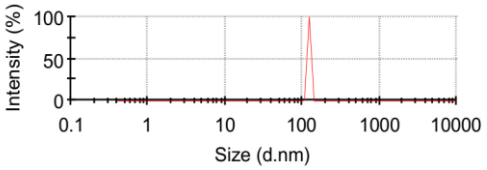

Figure 2. Size distribution of the milled graphite for 330 h

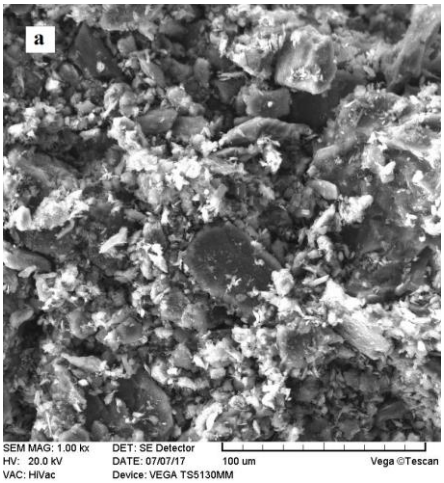

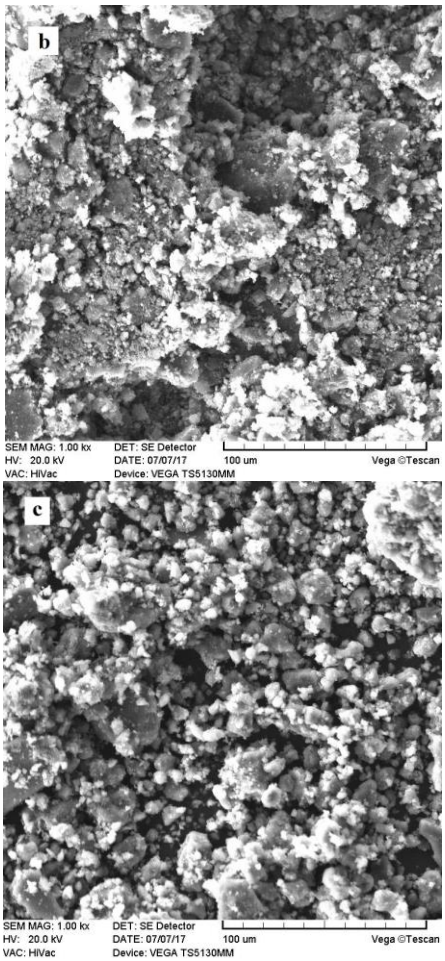

Figure 3. SEM images (a) initial graphite, (b) milled for 150 h, and (c)after 330 h of milling

EDX spectrum in Figure 4 reveals the different elements in the activated graphite for 330 h. These compositions such as iron contaminants play an important role in generating of CNTs, except the elements of Mg, Al, K, Ca, and Ti which come directly from the grid of SEM.

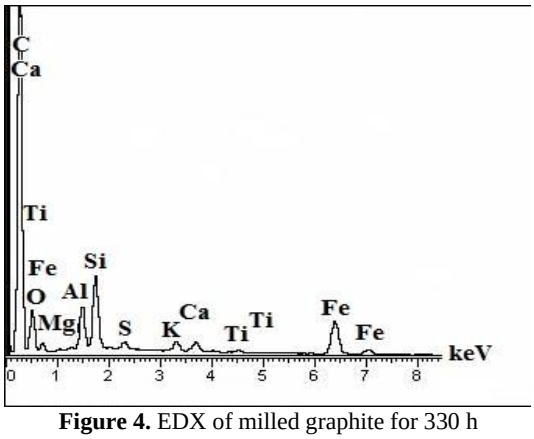

Figure 4. EDX of milled graphite for 330 h

TEM and AFM images of the fabricated CNTs after the thermal purification are demonstrated in Figure 5. The presence of a multitude number of carbon nanotubes in low magnification is a sign of the large-scale synthesis of the CNTs. The heat treatment and milling process are two major factors that determine the dimensions of the nanotubes. The distribution of 10-100 nm in diameter of carbon nanotubes and appropriate length (0.5-3 μm) indicate an approximately uniform size and dispersion of the metal catalyst particle which contaminates the powder during the ball milling process.

Nucleation and growth of CNTs are performing on catalyst particles according to the nucleation and the growth mechanism for the production of nanotubes in the presence of catalyst [26, 27]. By reducing the solubility and deposition of carbon atoms in the solution of carbon atoms and metal catalysts, carbon atoms by SP2 bonds are connected and finally, CNTs are formed. If carbon nanotubes grow upwards of the catalyst particles, the mechanism is labeled base-growth and if particles move at the head of the growing nanotubes, it is called tip-growth. Arrows in Figure 5 (c, d) illustrate catalyst particles that their possible endofullerenes and precipitates at the tips of the CNTs are obvious in the hypothetical tip-growth mechanism .

It seems during the mechanothermal process, first of all, amorphous carbons are attached to the catalyst particles and the nucleation stage is started. Next, the continuous longitudinal growth of nanotubes is taken by interfacial capillary forces and the diffusion of carbon atoms. Finally, the growth process continues as long as surface diffusion is supported by the concentration gradient and heat treatment. This finding corroborates the ideas of Chen et al. [16, 21] and Chadderton et al. [28]

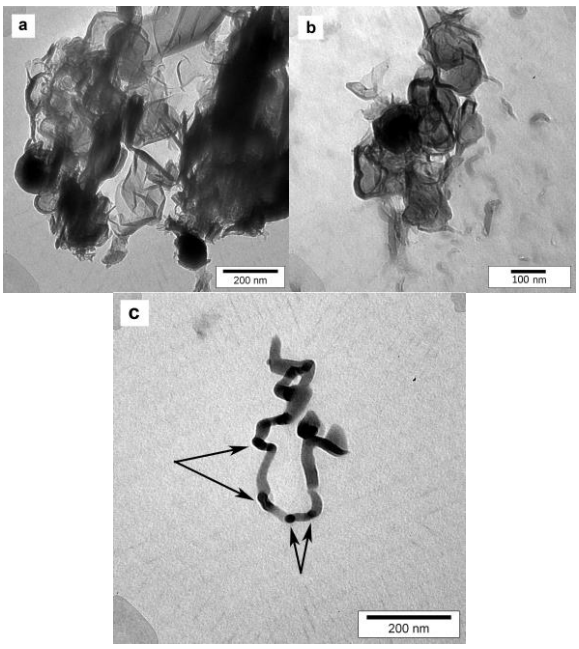

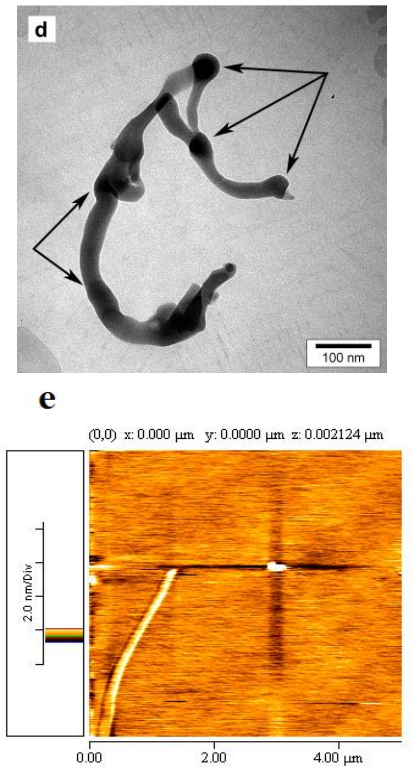

Figure 5. TEM (a, b, c, d, e) and AFM (d) images of synthesized carbon nanotubes by the heat treatment of ball-milled graphite after thermal purification (arrows show the catalyst particles)

who suggested that the growth of CNTs by the solid phase transformation is happened by surface diffusion. The growth of nanotubes entirely depends on the movement of the catalyst particle at the tip of the CNTs. Surface tensional forces, type, shape, and dimension of particle, heat and concentration gradient, and Van der Waals force between nanotubes are the most important factors which determine the direction of motion of the particle.

During the growth process, a competition between carbon atoms is created to form hexagons, heptagonal, and pentagons in the path of the particle. Hence, the length and width of the nanotubes are unpredictable and they are spring-like and bamboo-shaped with specific tubular hollow structures. The defects (heptagonal and pentagons) are preferred places for hydrogen storage [29-31]. As a result, synthesized curved nanotubes have a better performance for hydrogen storage compared to the straight nanotubes produced by other methods such as laser ablation or CVD. In addition, these manufactured nanotubes are probably more flexible than straight nanotubes and so they can be used for the production of high-strength nanocomposites by increasing the toughness of the matrix. Figure 6 provides information about the schematic diagram of the nucleation and growth of CNTs in the mechanothermal method .

The particles are larger than tubes and so it can therefore be assumed that the size of catalysts has a direct relationship with the diameter of the nanotubes, as previous reports [15, 32] confirmed an important impact of the milling time on the diameter of the CNTs. As a result, the long length and the relatively short diameter of the produced CNTs depict the usefulness of the long milling time and other applied factors in this study. Plus, furnace tube supplies the driving force for growing the nanotubes which this simple type of oven is economically more cost-effective than other methods such as laser ablation.

The X-ray diffraction pattern of the fabricated carbon nanotubes is shown in Figure 7. There are two main peaks. A sharp peak at 26˚ and a broad peak in the range of 41˚-43˚. According to Bragg's law [33], d002 was 0.342 nm, similar to d002 in multi-walled carbon nanotubes which is usually 0.34 nm [34].

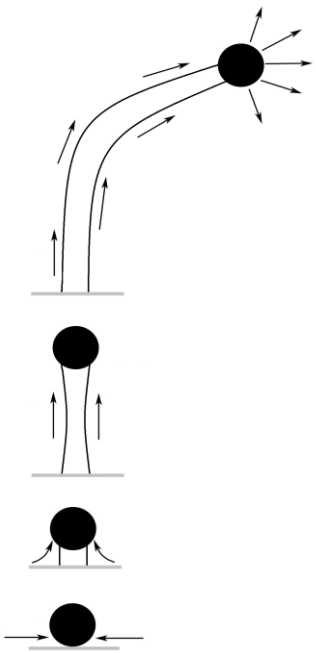

Figure 6. Schematic illustration of the proposed mechanism for the mechanothermal approach

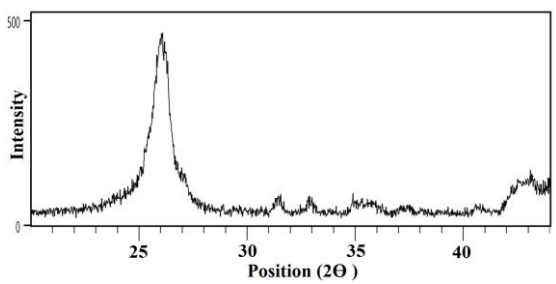

Figure 7. XRD diffraction pattern of the produced carbon nanotubes

In general, the d002 peak in CNTs is broadened, weakened, and shifted to the left side of the XRD profile by about half a degree (from 26.5˚ to 26˚), compared to pure graphite. This fact is related to the differences in the number of layers, changes in interlayer space, network distortion, and orientation of the carbon nanotubes against X-rays [35]. On the one hand, the diameter of the inner wall of multi-walled carbon nanotubes is more than 2 nm [36] and the obtained d002 is 0.342 nm. On the other, the number of walls usually has a one-to-one relationship with diameter according to Chiodarelli et al. [34]. As a result, it can be estimated that there are 20 to 50 walls in the synthesized CNT shown in Figure 5 with 20 nm in diameter. Overall, it is possible to hypothesize that a vast majority of the fabricated CNTs in this investigation have 10-40 walls, with attention to Chiodarelli's relation [34]. The strength of nanotubes is enhanced by increasing the number of walls whereas some of the other common methods such as laser ablation are unsuitable for the production of MWCNTs. Hence, the high number of walls of the prepared CNTs can makes them an ideal choice for the production of nanoalloys and nanocomposites.

Raman spectroscopy was performed for a more precise analysis of the quality and graphitization degree of the CNTs. The Raman spectra in Figure 8 indicate three main peaks. They are at 1349, 1566, and 2650 cm^{-1}, which are assigned to D, G, and G′ bands respectively. As well as, ID/IG and ID/IG′ were calculated 0.79 and 1.21, respectively.

The G-single-band (without Splitting) in Figure 8 is a strong sign of multi-walled carbon nanotubes. This fact is related to the non-split between G+ and G- bands due to the differences in the batches and diameters of MWCNTs [37]. The absence peak in radial breathing mode (100-200 cm^{-1}) is attributed to a large number of the walls (more than 20) and the inner diameter of CNTs (more than 2 nm), which make peaks immensely invisible and weak. The lack of any sharp peaks in this region shows a very small amount of generated single-walled carbon nanotubes (SWCNTs). D-band is concerned with asymmetry and disorders in the structure of graphite sheets including defects, impurities, and porosities that exist in carbon structures with sp2 hybridization [37-39]. The G′-band corresponds to the two-phonon process which its intensity depends on the purity of the sample and represents the long-range order of the CNTs [36, 40]. Thereby, ID/IG′ is a sensitive measure and less important than ID/IG for characterization of the quality and detecting the impurities of CNTs [41]. The obtained ID/IG and ID/IG′ ratios confirm ordered sp2 bonds and suitable quality of produced carbon nanotubes. It is also worth noting that the fabricated carbon nanotubes did not undergo any acid purification.

Figure 9 demonstrates the DTA/TGA analyses of the produced carbon nanotubes. The type of CNTs, quality,

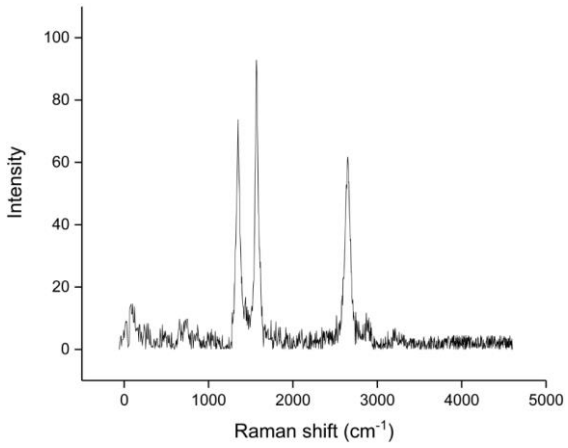

Figure 8. Raman spectrum of synthesized carbon nanotubes after thermal purification

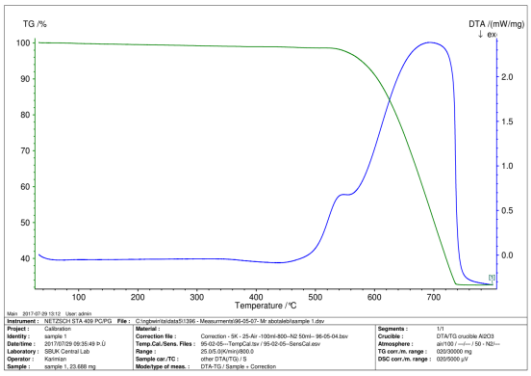

Figure 9. DTA/TG analyses of the fabricated CNTs

and purity of products can be determined regarding the initial temperature, oxidation temperature, residual mass, and weight loss in DTA/TGA. The oxidation temperature of amorphous carbon, SWCNTs, and MWCNTs are in the range of 200-300 ˚C, 350-500 ˚C, and 400-650 ˚C, respectively [36]. By comparing the weight percentage (vertical axis) and the temperatures (horizontal axis) with the mentioned oxidation temperature, the type and percentage of the produced nanotubes can be specified. As a consequence, one weight percentage of amorphous carbon, one weight percentage of single-walled carbon nanotubes, and more than 97 weight percentage of the initial amorphous carbon is converted to multi-walled carbon nanotubes .

The positive gradient in the DTA graph (450-700 ˚C) indicates the main exothermic reaction of MWCNTs with air. In some mechanothermal approaches, metal catalytic particles such as aluminum and yttrium, have been added to amorphous carbon to facilitate the fabrication of CNTs [42-44]. However, the obtained results show that the selected parameters without any additive catalyst are the optimal condition in the process .

On the one hand, common steel vials usually induce a lot of milling contaminants into the sample and the ceramic vials despite non-producing impurities, generates a small number of carbon nanotubes after heat treatment (due to non-metal catalyst) [43]. On the other hand, most of the elements in the chemical composition of the cup in this research including Fe, Si, S, Mn, Cr, and W were employed as the catalyst for the production of CNTs [17, 45-47]. Moreover, acid purification is a common step after the production of CNTs because it eliminates metal catalysts and increases the quality of nanotubes. Since no acid treatment was used in this study, a reasonable amount of iron contaminations is another sign of the appropriateness of the applied factors of milling. Especially when these results compare with other methods such as CVD which usually produce a very large percentage of metal impurities [3, 48]. Consequently, using this type of high-alloy steel in the vial, increasing the milling time, and selecting the different sizes of balls for complete amorphization of graphite, is proposed as a desirable way for the synthesizing of carbon nanotubes by the mechanothermal method.

4. CONCLUSION

In this study, by changing some effective variables in the mechanothermal approach, an attempt was made to optimize the efficiency of this method. First, the graphite powder was ball-milled for 330 h to maximize the amorphization. Subsequently, CNTs were produced by the annealing of amorphous carbon under the Ar atmosphere. A new tip-growth mechanism was recommend based on the random movement of the catalyst particles and it was shown that the direction of the growth does not follow a general movement according to the TEM images. The results of DTA/TG represent that by adjusting the effective variables, such as increasing milling time, select the appropriate temperature, using different sizes of the balls and special vial, mass production of carbon nanotubes (over 97%) is achieved by the mechanothermal way. This optimized method despite a long time of the process is very cost-effective and by applying the mentioned parameters, the quality and quantity of MWCNTs are increased simultaneously. The authors believe that this work has considerably developed the mechanothermal method and can be a starting point for future studies.

5. ACKNOWLEDGEMENTS

This study was funded by Shahid Bahonar University of Kerman and the author declares that they have no conflict of interest. It has not been published elsewhere and that it has not been submitted simultaneously for publication elsewhere.

6. REFERENCES

1. Chaudhary, S. and Singh, K., "Complex phenomenal growth of multi-walled carbon nanotubes in conventional arc discharge process", ***Transactions of the Indian Institute of Metals***, (2021), 1-6. DOI: 10.1007/s12666-021-02316-4
2. Ismail, R.A., Mohsin, M.H., Ali, A.K., Hassoon, K.I. and Erten-Ela, S., "Preparation and characterization of carbon nanotubes by pulsed laser ablation in water for optoelectronic application", ***Physica E: Low-dimensional Systems and Nanostructures***, Vol. 119, No. (2020), 113997. DOI: 10.1016/j.physe.2020.113997
3. Mirabootalebi, S.O. and Akbari, G.H., "Methods for synthesis of carbon nanotubes—review", ***International Journal of Bio-Inorganic Hybride Nanomaterials***, Vol. 6, No. 2, (2017), 49-57.
4. Li, Z., Yuan, D., Wu, H., Li, W. and Gu, D., "A novel route to synthesize carbon spheres and carbon nanotubes from carbon dioxide in a molten carbonate electrolyzer", ***Inorganic Chemistry Frontiers***, Vol. 5, No. 1, (2018), 208-216. DOI: 10.1039/C7QI00479F
5. Mirabootalebi, S., "A new method for preparing buckypaper by pressing a mixture of multi-walled carbon nanotubes and amorphous carbon", ***Advanced Composites and Hybrid Materials***, Vol. 3, No. 3, (2020), 336-343. DOI: 10.1007/s42114-020-00167-z
6. Manafi, S., Amin, M., Rahimipour, M., Salahi, E. and Kazemzadeh, A., "Large scale and low cost synthesis of multiwalled carbon nanotubes by mechanothermal absence catalysts", ***Advances in Applied Ceramics***, Vol. 109, No. 1, (2010), 25-30. DOI: 10.1179/174367609X414008
7. Manafi, S., Amin, M., Rahimipour, M., Salahi, E. and Kazemzadeh, A., "High-yield synthesis of multiwalled carbon nanotube by mechanothermal method", ***Nanoscale Research Letters***, Vol. 4, No. 4, (2009), 296-302. DOI: 10.1007/s11671-008-9240-3
8. Manafi, S., Rahimipour, M.R., Mobasherpour, I. and Soltanmoradi, A., "The synthesis of peculiar structure of springlike multiwall carbon nanofibers/nanotubes via mechanothermal method", ***Journal of Nanomaterials***, Vol. 2012, (2012), 15. DOI: 10.1155/2012/803546
9. Manafi, S., Rahimipour, M. and Soltanmoradi, A., "Ultra-high crystallinity millimeter long multiwall carbon nanotubes fabricated by mechanothermal method", ***Materials Science-Poland***, Vol. 30, No. 3, (2012), 226-230. DOI: 10.2478/s13536-012-0033-0
10. Boyrazlı, M. and Güler, S.H., "Synthesis of carbon nanostructures from corn stalk using mechano-thermal method", ***Journal of Molecular Structure***, Vol. 1199, (2020), 126976. DOI: 10.1016/j.molstruc.2019.126976
11. Chen, Y., Li, C.P., Chen, H. and Chen, Y., "One-dimensional nanomaterials synthesized using high-energy ball milling and annealing process", ***Science and Technology of Advanced Materials***, Vol. 7, No. 8, (2006), 839. DOI: 10.1016/j.stam.2006.11.014
12. Chen, Y., Fitz Gerald, J., Chadderton, L.T. and Chaffron, L., "Nanoporous carbon produced by ball milling", ***Applied Physics Letters***, Vol. 74, No. 19, (1999), 2782-2784. DOI: 10.1063/1.124012
13. Manafi, S., Amin, M., Rahimipour, M., Salahi, E. and Kazemzadeh, A., "Carbon nanotubes synthesized by mechanothermal method", ***New Carbon Materials***, Vol. 24, No. 1, (2009), 39-44. DOI: 10.1016/S1872-5805(08)60035-9
14. Güler, Ö. and Evin, E., "Carbon nanotubes formation by short-time ball milling and annealing of graphite", ***Optoelectronics and Advanced Materials***, Vol. 6, (2012), 183-187.
15. Evin, E., Güler, Ö., Aksoy, M. and Güler, S.H., "Effect of milling time on the formation of carbon nanotube by mechano-thermal

method", ***Bulletin of Materials Science***, Vol. 38, No. 4, (2015), 857-863. DOI: 10.1007/s12034-015-0952-6

16. Chen, Y., Conway, M., Gerald, J.F., Williams, J. and Chadderton, L., "The nucleation and growth of carbon nanotubes in a mechano-thermal process", ***Carbon***, Vol. 42, No. 8-9, (2004), 1543-1548. https://doi.org/10.1016/j.carbon.2004.02.003
17. Güler, Ö. and Evin, E., "Effect of milling type on formation of carbon nanostructures", ***Fullerenes, Nanotubes and Carbon Nanostructures***, Vol. 23, No. 5, (2015), 463-470.
18. Suryanarayana, C., "Mechanical alloying and milling", ***Progress in Materials Science***, Vol. 46, No. 1-2, (2001), 1-184.
19. Welham, N. and Williams, J., "Extended milling of graphite and activated carbon", ***Carbon***, Vol. 36, No. 9, (1998), 1309-1315. DOI: 10.1016/S0008-6223(98)00111-0
20. Li, J., Wang, L., Bai, G. and Jiang, W., "Carbon tubes produced during high-energy ball milling process", ***Scripta Materialia***, Vol. 54, No. 1, (2006), 93-97. DOI: 10.1016/j.scriptamat.2005.08.037
21. Chen, X., Yang, H., Wu, G., Wang, M., Deng, F., Zhang, X., Peng, J. and Li, W., "Generation of curved or closed-shell carbon nanostructures by ball-milling of graphite", ***Journal of Crystal Growth***, Vol. 218, No. 1, (2000), 57-61. DOI: doi.org/10.1016/S0022-0248(00)00486-3
22. Huang, Z., Calka, A. and Liu, H., "Effects of milling conditions on hydrogen storage properties of graphite", ***Journal of Materials Science***, Vol. 42, No. 14, (2007), 5437-5441.
23. Johan, M.R. and Moh, L.S., "Growth and optical study of carbon nanotubes in a mechano-thermal process", ***Carbon***, Vol. 8, (2013), 1047-1056.
24. Rietsch, J.-C., Gadiou, R., Vix-Guterl, C. and Dentzer, J., "The influence of the composition of atmosphere on the mechanisms of degradation of graphite in planetary ball millers", ***Journal of Alloys and Compounds***, Vol. 491, No. 1-2, (2010), L15-L19. DOI: 10.1016/j.jallcom.2009.10.193
25. Ong, T. and Yang, H., "Effect of atmosphere on the mechanical milling of natural graphite", ***Carbon***, Vol. 38, No. 15, (2000), 2077-2085. DOI: 10.1016/S0008-6223(00)00064-6
26. Purohit, R., Purohit, K., Rana, S., Rana, R. and Patel, V., "Carbon nanotubes and their growth methods", ***Procedia Materials Science***, Vol. 6, (2014), 716-728. DOI: 10.1016/j.mspro.2014.07.088
27. Lobo, L.S., "Nucleation and growth of carbon nanotubes and nanofibers: Mechanism and catalytic geometry control", ***Carbon***, Vol. 114, (2017), 411-417. https://doi.org/10.1016/j.carbon.2016.12.005
28. Chadderton, L.T. and Chen, Y., "A model for the growth of bamboo and skeletal nanotubes: Catalytic capillarity", ***Journal of Crystal Growth***, Vol. 240, No. 1-2, (2002), 164-169. https://doi.org/10.1016/S0022-0248(02)00855-2
29. Gayathri, V., Devi, N. and Geetha, R., "Hydrogen storage in coiled carbon nanotubes", ***international Journal of Hydrogen Energy***, Vol. 35, No. 3, (2010), 1313-1320. https://doi.org/10.1016/j.ijhydene.2009.11.083
30. Gayathri, V. and Geetha, R., "Hydrogen adsorption in defected carbon nanotubes", ***Adsorption***, Vol. 13, No. 1, (2007), 53-59. DOI: 10.1007/s10450-007-9002-z
31. Rajaura, R.S., Srivastava, S., Sharma, P.K., Mathur, S., Shrivastava, R., Sharma, S. and Vijay, Y., "Structural and surface modification of carbon nanotubes for enhanced hydrogen storage density", ***Nano-Structures & Nano-Objects***, Vol. 14, (2018), 57-65. https://doi.org/10.1016/j.nanoso.2018.01.005
32. Chen, Y., Conway, M. and Fitzgerald, J., "Carbon nanotubes formed in graphite after mechanical grinding and thermal annealing", ***Applied Physics A***, Vol. 76, No. 4, (2003), 633-636. https://doi.org/10.1007/s00339-002-1986-3
33. Ahmad, A., Pervaiz, M., Ramzan, S., Kiyani, M.Z., Khan, A., Ahmad, I. and Asiri, A.M., Role of xrd for nanomaterial analysis, in Nanomedicine manufacturing and applications. 2021, Elsevier.149-161. https://doi.org/10.1016/B978-0-12-820773-4.00008-1
34. Chiodarelli, N., Richard, O., Bender, H., Heyns, M., De Gendt, S., Groeseneken, G. and Vereecken, P.M., "Correlation between number of walls and diameter in multiwall carbon nanotubes grown by chemical vapor deposition", ***Carbon***, Vol. 50, No. 5, (2012), 1748-1752. DOI: 10.1016/j.carbon.2011.12.020
35. Mirabootalebi, S.O., Akbari Fakhrabadi, G.H. and Mirahmadi Babaheydari, R., "High-yield production of amorphous carbon via ball milling of graphite and prediction of its crystallite size through ann", ***Journal of Applied Organometallic Chemistry***, Vol. 1, No. 2, (2021), 76-85. http://dx.doi.org/10.22034/jaoc.2021.288020.1021
36. Lehman, J.H., Terrones, M., Mansfield, E., Hurst, K.E. and Meunier, V., "Evaluating the characteristics of multiwall carbon nanotubes", ***Carbon***, Vol. 49, No. 8, (2011), 2581-2602. https://doi.org/10.1016/j.carbon.2011.03.028I
37. Costa, S., Borowiak-Palen, E., Kruszynska, M., Bachmatiuk, A. and Kalenczuk, R., "Characterization of carbon nanotubes by raman spectroscopy", ***Materials Science-Poland***, Vol. 26, No. 2, (2008), 433-441.
38. Benoit, J., Buisson, J., Chauvet, O., Godon, C. and Lefrant, S., "Low-frequency raman studies of multiwalled carbon nanotubes: Experiments and theory", ***Physical Review B***, Vol. 66, No. 7, (2002), 073417. https://doi.org/10.1103/PhysRevB.66.073417
39. Antunes, E., Lobo, A., Corat, E. and Trava-Airoldi, V., "Influence of diameter in the raman spectra of aligned multi-walled carbon nanotubes", ***Carbon***, Vol. 45, No. 5, (2007), 913-921. https://doi.org/10.1016/j.carbon.2007.01.003
40. DiLeo, R.A., Landi, B.J. and Raffaelle, R.P., "Purity assessment of multiwalled carbon nanotubes by raman spectroscopy", ***Journal of Applied Physics***, Vol. 101, No. 6, (2007), 064307. https://doi.org/10.1063/1.2712152
41. Chakrapani, N., Curran, S., Wei, B., Ajayan, P.M., Carrillo, A. and Kane, R.S., "Spectral fingerprinting of structural defects in plasma-treated carbon nanotubes", ***Journal of Materials Research***, Vol. 18, No. 10, (2003), 2515-2521. https://doi.org/10.1557/JMR.2003.0350
42. Connan, H.G., Reedy, B.J., Marshall, C.P. and Wilson, M.A., "New nanocarbons: Rod milling and annealing of graphite in the presence of yttrium", ***Energy & Fuels***, Vol. 18, No. 6, (2004), 1607-1614. https://doi.org/10.1021/ef0400114
43. Rosas, G., Esparza, R., Liu, H., Ascencio, J. and Pérez, R., "Mechanical alloying synthesis of carbon nanotubes in the presence of alfe small clusters", ***Materials Letters***, Vol. 61, No. 3, (2007), 860-863. DOI: 10.1016/j.matlet.2006.06.032
44. Khazaei Feizabad, M., Khayati, G.R. and Pouresterabadi, S., "Design and synthesis of carbon nanotubes for adsorption utilities: An approach to direct preparation by mechanical milling at room temperature", ***Scientia Iranica***, Vol. 28, No. 3, (2021), 1884-1895. DOI: 10.24200/sci.2020.52977.2979
45. Das, D. and Roy, A., "Synthesis of diameter controlled multiwall carbon nanotubes by microwave plasma-cvd on low-temperature and chemically processed fe nanoparticle catalysts", ***Applied Surface Science***, Vol. 515, (2020), 146043. https://doi.org/10.1016/j.apsusc.2020.146043
46. Shah, K.A., Najar, F.A., Sharda, T. and Sreenivas, K., "Synthesis of multi-walled carbon nanotubes by thermal cvd technique on pt–w–mgo catalyst", ***Journal of Taibah University for Science***, Vol. 12, No. 2, (2018), 230-234. https://doi.org/10.1080/16583655.2018.1451114
47. Wang, J., Wang, W., Li, H., Tan, T., Wang, X. and Zhao, Y., "Carbon nanotubes/sic prepared by catalytic chemical vapor

deposition as scaffold for improved lithium-sulfur batteries", ***Journal of Nanoparticle Research***, Vol. 21, No. 6, (2019), 1-10. Doi:10.1007/s11051-019-4540-3

48. Aminayi, P., Allaedini, G. and Tasirin, S.M., "Hydrodynamic studies of fluidized bed chemical vapor deposition reactors to produce carbon nano tubes via catalytic decomposition over co/pd mgo", ***International Journal of Engineering***, Vol. 28, No. 12, (2016), 1693-1701. Doi: 10.5829/idosi.ije.2015.28.12c.01

Persian Abstract

چکیده

مولفه های موثر فراوانی در فرآیند مکانوترمال موثرند که عبارتند از سرعت آسیاب، نسبت اندازه گلوله به پودر و غیره. این موارد در کیفیت و کمیت نانولوله های کربنی تولیدی نقشی مهم دارند. در تحقیق پیش رو سعی شد تا با بهینه کردن پارامترهای اساسی؛ کیفیت ناتولوله های تولیدی افزایش یابد و همچنین مکانیزم رشد نانولوله ها نیز بررسی شد. بدین منظور آسیاکاری گرافیت در آسیاب گلوله ای و در کاپ با استاندارد ۱.۲۵۵۰ کلید فولاد انجام شد. سپس، ساختار ذرات آسیاکاری شده با آنالیزهایی نظیر زتاسایزر، میکروسکوپ الکترونی روبشی بررسی شدند. در گام بعدی، این پدرها تحت عملیات حرارتی در ۱۴۰۰ درجه سانتیگراد قرار گرفتند تا نانولوله های کربنی تولید شدند. مدلی خاص از رشد (tip-growth) بر اساس آنالیزهای محصولات فرآیند ارایه شد و همچنین راندمان روش بهینه شده مورد ارزیابی قرار گرفت.